ACS Photonics

Article

pubs.acs.org/journal/apchd5

Quantum Effects in Charge Transfer Plasmons

Vikram Kulkarni and Alejandro Manjavacas*

Department of Physics and Astronomy and Laboratory for Nanophotonics, Rice University, 6100 Main Street, Houston, Texas 77005, United States

Supporting Information

ABSTRACT: Metallic nanoparticles placed in close proximity support strong localized surface plasmon resonances. One such resonance, known as the charge transfer plasmon, involves the physical transfer of electrons between the nanoparticles and, thus, exists only in dimers bridged with conductive junctions. Here we analyze the quantum effects associated with these type of plasmon modes by studying the optical response of a metallic dimer bridged with a two-level system. We find that the charge transfer plasmons are observed in the absorption spectrum only when one of the energy levels of the two-level system is resonant with the Fermi level of the nanoparticles. Furthermore, we explicitly show that, for the resonant configuration, the conductance of the junction reaches a value equal to one quantum of conductance, $2e^2/h$. Our results establish a connection between the optical response of plasmonic nanostructures and quantum transport phenomena, thus bringing a new perspective to quantum plasmonics.

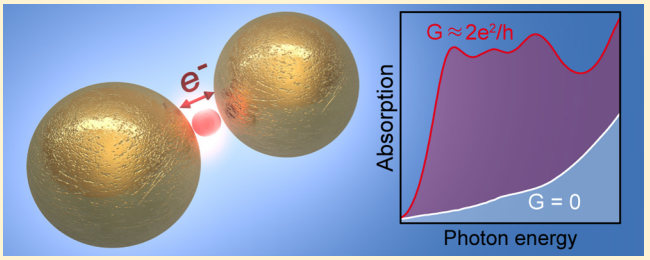

KEYWORDS: *surface plasmon, charge transfer plasmon, quantum plasmonics, quantum transport, quantum junction, metallic dimer, time-dependent density functional theory (TDDFT), two-level system*

Surface plasmons, the collective oscillations of the conduction electrons of metallic nanostructures, have been the subject of extensive investigation in the past years due to their extraordinary ability to confine electromagnetic energy into subwavelength spatial regions, and therefore to produce strong near fields.[1,2] These properties have been exploited to develop applications as diverse as photothermal cancer therapies,[3,4] ultrasensitive sensors,[5,6] or enhanced photovoltaic devices.[7,8] Surface plasmons are commonly described through classical approaches based on solving Maxwell's equations using local dielectric functions. However, these approaches fail when dealing with nanostructures with length scales on the order of a few nanometers.[9] In those cases, a more elaborate description has proved necessary to understand effects related to size quantization,[10−17] nonlocality,[18−24] or tunneling,[25−29] which emerge from the quantum nature of the conduction electrons. To that end, different approaches based on, for instance, the time-dependent density functional theory (TDDFT)[11,25,26,30,31] or hydrodynamic models[19,24,32] have been developed.

The advances in the nanofabrication techniques have allowed the experimental verification of some of the predicted quantum plasmonic effects in systems involving individual nanoparticles,[33,34] particles coupled to metallic films,[35,36] or closely spaced dimers.[37−39] Indeed, the dimer geometry is very well suited to observe the quantum nature of plasmons due the strong near fields at the gap and the possibility of electron tunneling. Metallic dimers are well known to support a strongly radiative mode known as the bonding dipolar plasmon (BDP)[40,41] consisting of an in-phase oscillation of the individual nanoparticle dipolar plasmons.[42] Additionally, another mode known as the charge transfer plasmon (CTP) appears at low energy when the two particles of the dimer are connected through a conductive junction.[26,38,43−45] This mode involves a substantial current flowing between the nanoparticles via the junction, which results in the particles exhibiting a net charge of opposite sign. For that reason, the CTPs are sometimes thought of as a hybridization of monopole modes.[46]

A classical description of these resonances involves the solution of Maxwell's equations with the junction modeled using a finite conductivity that is plugged into the dielectric function.[43] Although this approach leads to accurate results for bulky junctions,[47,48] it cannot completely describe the behavior of dimers bridged by quantum systems, such as atoms[49,50] or molecules.[51,52] In those cases, the discrete electronic structure of the junction strongly influences the optical response of the metallic dimer, as it has been recently shown experimentally.[53]

In this paper we investigate the quantum effects associated with the CTPs through the analysis of the optical response of a small metallic dimer bridged with a two-level system (TLS, e.g., an atom, a molecule, or a quantum dot). Using a fully quantum approach, we calculate the absorption spectrum of the system and correlate it to the electronic structure of the junction. Our results show that a CTP appears in the spectrum only when an energy level of the TLS is resonant with the Fermi level of the metallic nanoparticles, thus enabling the flow of electrons through the junction. Furthermore, by explicitly calculating the

Received: May 7, 2015
Published: June 25, 2015

DOI: 10.1021/acsphotonics.5b00246
ACS Photonics 2015, 2, 987−992

conductance of the junction, we find that, for the resonant configuration, this quantity reaches a value equal to one quantum of conductance, $G_0 = 2e^2/h$. The results presented in this work bring a new perspective to the investigation of the quantum effects in the plasmonic response of metallic nanoparticles by shedding light on their connection with quantum transport phenomena.

RESULTS AND DISCUSSION

The system under study is depicted in Figure 1a. We consider a metallic dimer composed of two identical gold nanoparticles with a diameter of 32 au, separated by a gap of 8 au, in which a TLS is placed in order to form a junction. The latter is modeled as a small sphere of 6 au in diameter and simulates an atom, a molecule, or a quantum dot. The whole structure is embedded in vacuum and possesses cylindrical symmetry about the z-axis. In order to analyze the behavior of this system, we use a fully quantum approach based on the TDDFT[54−56] in the adiabatic local density approximation,[57,58] which has been successfully used in previous investigations of the plasmonic response of metallic nanostructures.[11,12,14,25,27] We consider only the conduction electrons of the metal and model the metallic nanoparticles within the jellium approximation, in which the ionic background charge is replaced by an uniform charge density n_0. The value of n_0 is chosen to match the density of gold, which corresponds to a Wigner−Seitz radius of 3 au. The same procedure is used to model the TLS, whose radius is chosen equal to the Wigner−Seitz radius. This ensures that the TLS adds a single electron to the system. In the absence of external fields the effective one-electron potential is then given by

$$V_{\mathrm{eff}}(\mathbf{r}) = V_0(\mathbf{r}) + V_{\mathrm{H}}[n(\mathbf{r}) - n_0(\mathbf{r})] + V_{\mathrm{xc}}[n(\mathbf{r})]$$

where V_{H} is the Hartree potential, n is the electronic density, n_0 is the background ionic charge density, and V_{xc} is the exchange−correlation potential, corresponding to the Perdew−Zunger functional within the local density approximation.[58] V_0 represents a uniform background potential terminating at the surfaces of the nanostructures that confines the electrons to the nanoparticles and the TLS. For the nanoparticles, the value of this potential is fixed at −4.6 eV in order to ensure a reasonable position of the Fermi energy of the system (5.2 eV below the vacuum level) and therefore to obtain the appropriate electron spill-out. On the contrary, the value of the background potential for the TLS is left as a parameter, V_{TLS} (see Figure 1b). This allows us to control the position of the energy levels of the TLS with respect to the Fermi level of the nanoparticles. Further details on the theoretical approach can be found in the Supporting Information.

Figure 1b shows the background potential (gray line) and the resulting equilibrium one-electron potential (red line) plotted along the dimer axis (z-axis), for the particular case in which $V_{\mathrm{TLS}} = -4.6$ eV (see Figure S1 in the Supporting Information for other values of V_{TLS}). As a consequence of this election, the depth of the one-electron potential at the TLS is nearly the same as at the nanoparticles. Furthermore, the presence of the TLS clearly lowers the potential barrier of the junction, leaving it slightly above the Fermi level of the system (black dashed line). For values of $|z| > 36$ au the potential rises sharply to zero, thus confining all electrons to within the nanoparticles

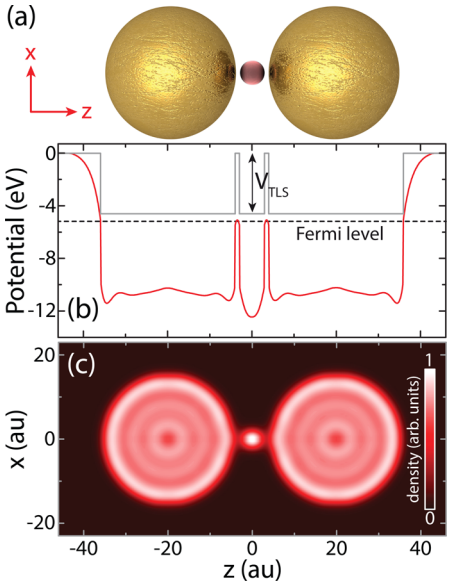

Figure 1. Description of the system under study. (a) A spherical two-level system (TLS, e.g., an atom, a molecule, or a quantum dot) with a diameter of 6 au is placed between two metallic nanoparticles with a diameter of 32 au separated by a gap of 8 au. (b) Equilibrium one-electron potential (red line) and background potential (gray line), both plotted along the dimer axis for the case in which the background potential of the TLS is $V_{\mathrm{TLS}} = -4.6$ eV. The Fermi level of the nanostructure is shown by a dashed black line (−5.2 eV). (c) Equilibrium electronic density of the system on the xz-plane for the same situation as in panel (b).

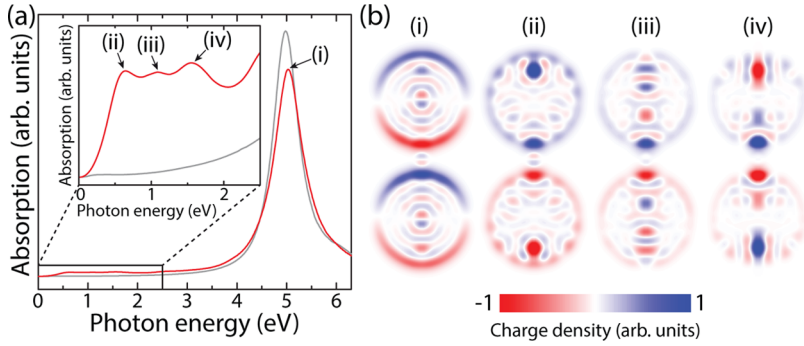

Figure 2. Optical response of the system under study. (a) Absorption spectrum for the bare metallic dimer (gray line) and for the dimer with the TLS (red line). In the second case we choose $V_{\mathrm{TLS}} = -4.6$ eV. The inset shows a zoom-in of the low-energy region. (b) Snapshots of the induced charge distributions calculated at photon energies of (i) 5.05 eV, (ii) 0.65 eV, (iii) 1.10 eV, and (iv) 1.55 eV.

DOI: 10.1021/acsphotonics.5b00246
ACS Photonics 2015, 2, 987−992

and the TLS. The corresponding equilibrium electronic density is plotted in Figure 1c for the *xz*-plane. It clearly shows Friedel oscillations over the whole volume of the nanoparticles. This is a direct consequence of the small size of the system, which leads to a discretization of the electronic levels. For larger systems, with a less discretized density of states, the electronic density is smoother within the nanoparticle, with salient Friedel oscillations remaining only near the surfaces.[11,15] On the other hand, the electronic density in the junction shows the occupation of a single energy level of the TLS. Interestingly, due to the lowering of the potential barrier caused by the TLS, the electronic density in the gaps between the particles and the TLS does not drop to zero.

Once the ground state of the system is known, we can compute its optical properties using the random phase approximation within the linear response theory[59] (see the Supporting Information for more details). For the sake of simplicity we neglect the background polarizability of the metal and focus on the effects mediated by the conduction electrons. We choose the external field to be polarized along the *z*-axis and assume that it is uniform over the extension of the nanostructure, which is justified by the small size of the latter. Figure 2a shows the absorption spectrum for the bare metallic dimer (gray line) and for the dimer with the TLS (red line) placed at the gap. In the second situation, we choose the background potential of the TLS to be equal to that of the nanoparticles (i.e., $V_{TLS} = -4.6$ eV). In both cases, the high-energy part of the spectrum is dominated by a BDP that appears at 5.05 eV. The nature of this mode is confirmed by the induced charge distribution plotted in Figure 2b(i), which displays a clear dipolar pattern on the surface of each of the nanoparticles.

The situation is very different for the low-energy part of the spectrum. As shown in the inset of Figure 2a, a set of three new peaks emerge in this region when the TLS is placed at the gap. Similar resonances have been also observed in previous works analyzing the response of a nanoparticle dimer bridged with a sodium atom.[49] Examining the corresponding induced charge distributions shown in Figure 2b(ii)−(iv), we observe that the three modes display a monopolar pattern on the surface of the particles. Interestingly, modes (iii) and (iv) also show an oscillation of charge inside the sphere most likely due to finite size effects. The monopolar pattern is a signature of the flow of charge through the junction associated with a CTP mode and is in stark contrast to the BDP mode, for which each nanoparticle remains charge neutral (cf. Figure 2b(i)).

The excitation of a CTP requires the transfer of charge from one particle of the dimer to the other. The results plotted in Figure 2a show that, in spite of the small interparticle distance of our system, the direct tunneling of electrons across the gap does not provide enough charge flow to sustain a CTP (cf. red and gray lines). This means that the only possible mechanism leading to the excitation of a CTP in our structure involves the use of the levels of the TLS as the conductive channels that allow the electrons to flow across the junction (see the sketch shown in Figure 3a). Therefore, we expect the existence of the CTP to be determined by the position of the levels of the TLS relative to the Fermi level of the nanostructure. In order to confirm this hypothesis, we analyze the response of the system for different values of the background potential of the TLS, V_{TLS}. As shown in Figure 3b, the variation of this parameter allows us to control the position of the levels of the TLS. Each dot in that plot represents an energy level of the whole

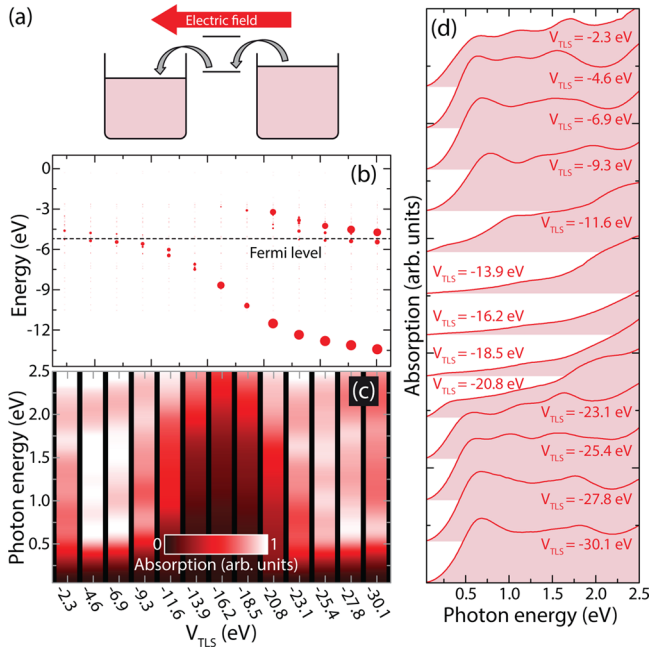

Figure 3. Interplay between the charge transfer plasmon and the electronic structure of the nanostructure. (a) Schematic of the physical mechanism leading to a CTP. (b) Electronic structure of the system as a function of the background potential of the TLS, V_{TLS}. Each dot represents an energy level of the system, while its size is proportional to the localization of that level on the TLS. The black dashed line indicates the Fermi level of the system (−5.2 eV). (c, d) Absorption spectrum of the system as a function of V_{TLS} plotted in two different formats.

nanostructure. The size of the dot is proportional to the degree of localization of that level on the TLS, which is calculated by integrating the squared modulus of the corresponding wave function over the volume of the TLS, $\int_{TLS} d\mathbf{r}|\Psi(\mathbf{r})|^2$, and allows us to distinguish the levels localized in the TLS from the rest of the states.

For small values of V_{TLS}, we find a group of states localized in the TLS, all of them with energies close to the Fermi level of the system (black dashed line). These states originate from the splitting of the ground state of the TLS due to the interaction with the nanoparticles. As the background potential becomes deeper, the states move down in the energy diagram and become more localized on the TLS, as seen from the increase of the dot size. Interestingly, due to the stronger localization, the interaction with the nanoparticles is reduced, and therefore the splitting disappears. For $V_{TLS} < -16.2$ eV a second level localized on the TLS emerges at high energies, which corresponds to the excited state of the TLS. Again, the interaction with the nanoparticles splits this state into a few states with very close energies. It is important to note that here we modify only V_{TLS}; the geometry and aspect ratio of the overall system remain constant in all cases.

Figure 3c and d show the low-energy part of the absorption spectrum of the system calculated for the different values of V_{TLS} considered in panel b. These results clearly show that the CTP modes appear in the spectrum only when there is a state localized in the TLS whose energy is close to the Fermi level of the system, thus confirming our initial hypothesis. This is clearly the case for $V_{TLS} = -4.6$ eV, in which the presence of two states, localized in the TLS, around the Fermi level results in the strong absorption spectrum that was discussed in Figure

DOI: 10.1021/acsphotonics.5b00246
ACS Photonics 2015, 2, 987−992

2. As V_{TLS} takes more negative values, and therefore the states localized in the TLS move away from the Fermi level, the CTP modes disappear and the spectrum becomes featureless. The weakest absorption is obtained for $V_{TLS} = -16.2$ eV, coinciding with a situation in which the Fermi level lies midway between the ground and the excited TLS states. The CTP modes reappear in the spectrum only for $V_{TLS} < -23.1$ eV, when the excited TLS state moves close enough to the Fermi level.

We can complete the characterization of our system and get a better understanding of the CTP modes by calculating explicitly the conductance of the junction. In order to do so, first we obtain the total charge that flows through the junction by integrating the induced charge density over the volume of one of the metallic spheres. The results of this calculation are plotted in Figure 4a (red line) as a function of the background

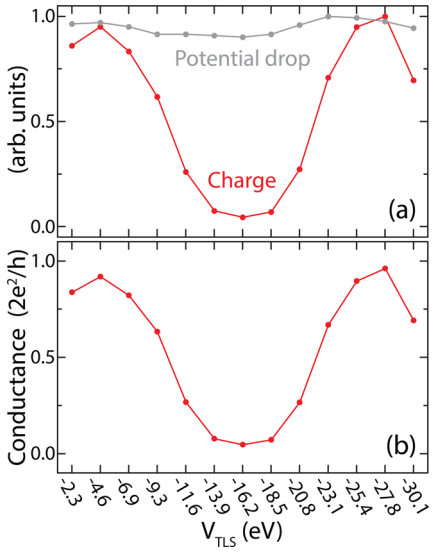

Figure 4. Transport properties of the junction. (a) Induced charge on one of the nanoparticles (red line) and induced potential drop calculated at the inner surfaces of the nanoparticles on opposite sides of the junction (gray line). Both quantities are plotted as a function of the background potential of the TLS, V_{TLS}. (b) Conductance of the junction in units of the quantum of conductance, $G_0 = 2e^2/h$, also as a function of V_{TLS}. In all cases we assume a photon energy of 0.65 eV.

potential of the TLS. In all cases we assume a photon energy of 0.65 eV. As expected, the charge is accumulated in the particles for the values of V_{TLS} for which we observe the CTP modes in the spectrum, while its value drops to zero for $V_{TLS} = -16.2$ eV, exactly when the low-energy part of the absorption spectrum turns featureless (cf. Figure 3c and d). Once the charge is known, and since we are working in the frequency domain, the current flowing through the junction is obtained by multiplying the charge by $i\omega$, where ω is the oscillation frequency. Figure 4a also shows the potential drop built in the junction (gray line), calculated at the surface of the nanoparticles on opposite sides of the junction. This quantity, which is obtained from Poisson's equation using the induced charge, shows a dependence similar to the charge, although its value remains almost constant as V_{TLS} is varied.

The conductance is then calculated as the ratio between the current and the potential drop across the junction. We plot this quantity in Figure 4b as a function of V_{TLS}. It clearly follows the same dependence as the charge; namely, the conductance is significant only when a level localized in the TLS is resonant with the Fermi energy of the nanoparticles. For small V_{TLS}, only the ground state of the TLS contributes to the conductance. In contrast, when V_{TLS} becomes more negative, the conductance is solely due to the TLS excited state. But when neither the ground state nor the excited state is resonant with the Fermi level (as is the case for $V_{TLS} = -16.2$ eV), the conductance drops to zero. Interestingly, in the resonant condition, this quantity reaches a value equal to one quantum of conductance, $G_0 = 2e^2/h$. This fact, which is not surprising since there is only one level available to the electrons to cross the junction, is a clear signature of the quantum character of this system. Furthermore, it suggests that the contact resistance between the TLS and the metallic nanoparticles is zero, which is consistent with the small potential barrier existing between the TLS and the nanoparticles as shown in Figure S1 of the Supporting Information. If we add more levels to the junction, either by having a bridging element with a more complex electronic structure or by having multiple TLS in the gap, the maximum conductance will be increased, eventually reaching a classical behavior.[52]

CONCLUSIONS

In summary, we have studied the quantum properties of the CTPs supported by a metallic dimer bridged with a TLS, representing an atom, a molecule, or a quantum dot. Using a fully quantum approach based on the TDDFT, we have been able to correlate the absorption spectrum of this system with the electronic structure of the junction. We have found that a CTP can be observed in the spectrum only when an energy level of the TLS is resonant with the Fermi level of the metallic nanoparticles. This demonstrates that the existence of the CTP is determined by the electronic structure of the junction, in clear agreement with recent experimental works.[53] Furthermore, by explicitly calculating the conductance of the junction, we have shown that in the resonant configuration this quantity reaches a value equal to one quantum of conductance, $G_0 = 2e^2/h$. Although our simulations have been performed for small systems containing ~300 electrons, we expect our results to hold for much larger systems, but the quantum character of the junction will be lost if the number of conduction channels in the junction becomes sufficiently large. An experimental verification of our theoretical predictions would require the tuning of the electronic levels of the junction. This can be done in various ways; one possibility is to load the junction with molecular species having different HOMO−LUMO gaps.[53] An alternative path is to rely on externally applied static electric or magnetic fields to modify the electronic structure of the junction.[60] Additionally the Fermi energy of the nanoparticles can be changed by using metals with different work functions. All our calculations have been performed within the linear response theory. However, for large applied fields the system is likely to exhibit nonlinear behaviors, including the possibility of direct tunneling of electrons between the two nanoparticles.[48,61] The results presented here establish a new connection between the plasmonic response of metal nanostructures and quantum transport phenomena, thus bringing a new perspective to the emerging field of quantum plasmonics, which may enable the development of new applications in nanophotonics and optoelectronics.

DOI: 10.1021/acsphotonics.5b00246
ACS Photonics 2015, 2, 987−992

■ ASSOCIATED CONTENT

Supporting Information

We provide a description of the theoretical formalism used in this work and the background and the equilibrium one-electron potentials for different V_{TLS}. The Supporting Information is available free of charge on the ACS Publications website at DOI: 10.1021/acsphotonics.5b00246.

■ AUTHOR INFORMATION

Corresponding Author

*E-mail: alejandro.manjavacas@rice.edu.

Notes

The authors declare no competing financial interest.

■ ACKNOWLEDGMENTS

We thank Dr. Peter Nordlander for helpful and enjoyable discussions and Dr. Jorge Zuloaga for his help with the numerical implementation of the TDDFT approach. This work was supported in part by the Cyberinfrastructure for Computational Research funded by NSF under Grant CNS-0821727. A.M. acknowledges support from the Welch Foundation under the J. Evans Attwell-Welch Fellowship for Nanoscale Research, administrated by the Richard E. Smalley Institute for Nanoscale Science and Technology (Grant L-C-004).

■ REFERENCES

(1) Maier, S. A. *Plasmonics: Fundamentals and Applications*; Springer: New York, 2007.

(2) Novotny, L.; Hecht, B. *Principles of Nano-Optics*; Cambridge University Press: New York, 2006.

(3) O'Neal, D. P.; Hirsch, L. R.; Halas, N. J.; Payne, J. D.; West, J. L. Photo-Thermal Tumor Ablation in Mice Using Near Infrared-Absorbing Nanoparticles. *Cancer Lett.* **2004**, *209*, 171−176.

(4) Lal, S.; Clare, S. E.; Halas, N. J. Nanoshell-enabled photothermal cancer therapy: impending clinical impact. *Acc. Chem. Res.* **2008**, *41*, 1842−1851.

(5) Xu, H.; Bjerneld, E. J.; Käll, M.; Börjesson, L. Spectroscopy of single hemoglobin molecules by surface enhanced Raman scattering. *Phys. Rev. Lett.* **1999**, *83*, 4357−4360.

(6) Anker, J. N.; Hall, W. P.; Lyandres, O.; Shah, N. C.; Zhao, J.; Van Duyne, R. P. Biosensing with plasmonic nanosensors. *Nat. Mater.* **2008**, *7*, 442−453.

(7) Catchpole, K. R.; Polman, A. Plasmonic solar cells. *Opt. Express* **2008**, *16*, 21793−21800.

(8) Atwater, H. A.; Polman, A. Plasmonics for improved photovoltaic devices. *Nat. Mater.* **2010**, *9*, 205−213.

(9) Tame, M. S.; McEnery, K. R.; Ozdemir, S. K.; Lee, J.; Maier, S. A.; Kim, M. S. Quantum plasmonics. *Nat. Phys.* **2013**, *9*, 329−340.

(10) Halperin, W. P. Quantum size effects in metal particles. *Rev. Mod. Phys.* **1986**, *58*, 533−606.

(11) Prodan, E.; Nordlander, P. Electronic Structure and Polarizability of Metallic Nanoshells. *Chem. Phys. Lett.* **2002**, *352*, 140−146.

(12) Zuloaga, J.; Prodan, E.; Nordlander, P. Quantum plasmonics: Optical properties and tunability of metallic nanorods. *ACS Nano* **2010**, *4*, 5269−5276.

(13) Townsend, E.; Bryant, G. W. Plasmonic properties of metallic nanoparticles: the effects of size quantization. *Nano Lett.* **2012**, *12*, 429−434.

(14) Zhang, H.; Kulkarni, V.; Prodan, E.; Nordlander, P.; Govorov, A. O. Theory of quantum plasmon resonances in doped semiconductor nanocrystals. *J. Phys. Chem. C* **2014**, *118*, 16035−16042.

(15) Manjavacas, A.; García de Abajo, F. J. Tunable plasmons in atomically thin gold nanodisks. *Nat. Commun.* **2014**, *5*, 3548.

(16) Zhang, P.; Feist, J.; Rubio, A.; García-González, P.; García-Vidal, F. J. Ab *initio* nanoplasmonics: The impact of atomic structure. *Phys. Rev. B: Condens. Matter Mater. Phys.* **2014**, *90*, 161407.

(17) Barbry, M.; Koval, P.; Marchesin, F.; Esteban, R.; Borisov, A. G.; Aizpurua, J.; Sánchez-Portal, D. Atomistic near-field nanoplasmonics: reaching atomic-scale resolution in nanooptics. *Nano Lett.* **2015**, *15*, 3410.

(18) García de Abajo, F. J. Nonlocal effects in the plasmons of strongly interacting nanoparticles, dimers, and waveguides. *J. Phys. Chem. C* **2008**, *112*, 17983−17987.

(19) David, C.; García de Abajo, F. J. Spatial nonlocality in the optical response of metal nanoparticles. *J. Phys. Chem. C* **2011**, *115*, 19470−19475.

(20) Wiener, A.; Fernández-Domínguez, A. I.; Horsfield, A. P.; Pendry, J. B.; Maier, S. A. Nonlocal effects in the nanofocusing performance of plasmonic tips. *Nano Lett.* **2012**, *12*, 865−871.

(21) Teperik, T. V.; Nordlander, P.; Aizpurua, J.; Borisov, A. G. Quantum effects and nonlocality in strongly coupled plasmonic nanowire dimers. *Opt. Express* **2013**, *21*, 27306−27325.

(22) Luo, Y.; Fernandez-Dominguez, A. I.; Wiener, A.; Maier, S. A.; Pendry, J. B. Surface Plasmons and Nonlocality: A Simple Model. *Phys. Rev. Lett.* **2013**, *111*, 093901.

(23) Christensen, T.; Yan, W.; Raza, S.; Jauho, A.-P.; Mortensen, N. A.; Wubs, M. Nonlocal response of metallic nanospheres probed by light, electrons, and atoms. *ACS Nano* **2014**, *8*, 1745−1758.

(24) Mortensen, N. A.; Raza, S.; Wubs, M.; Søndergaard, T.; Bozhevolnyi, S. I. A generalized non-local optical response theory for plasmonic nanostructures. *Nat. Commun.* **2014**, *5*, 3809.

(25) Zuloaga, J.; Prodan, E.; Nordlander, P. Quantum description of the plasmon resonances of a nanoparticle dimer. *Nano Lett.* **2009**, *9*, 887−891.

(26) Esteban, R.; Borisov, A. G.; Nordlander, P.; Aizpurua, J. Bridging quantum and classical plasmonics with a quantum-corrected model. *Nat. Commun.* **2012**, *3*, 825.

(27) Kulkarni, V.; Prodan, E.; Nordlander, P. Quantum plasmonics: optical properties of a nanomatryushka. *Nano Lett.* **2013**, *13*, 5873−5879.

(28) Marinica, D. C.; Lourenço-Martins, H.; Aizpurua, J.; Borisov, A. G. Plexciton quenching by resonant electron transfer from quantum emitter to metallic nanoantenna. *Nano Lett.* **2013**, *13*, 5972−5978.

(29) Esteban, R.; Zugarramurdi, A.; Zhang, P.; Nordlander, P.; Garcia-Vidal, F. J.; Borisov, A. G.; Aizpurua, J. A classical treatment of optical tunneling in plasmonic gaps: extending the quantum corrected model to practical situations. *Faraday Discuss.* **2015**, *178*, 151−183.

(30) Castro, A.; Marques, M. A. L.; Alonso, J. A.; Rubio, A. Optical properties of nanostructures from time-dependent density functional theory. *J. Comput. Theor. Nanosci.* **2004**, *1*, 231−255.

(31) Aikens, C. M.; Li, S.; Schatz, G. C. From discrete electronic states to plasmons: TDDFT optical absorption properties of Ag n (n = 10, 20, 35, 56, 84, 120) tetrahedral clusters. *J. Phys. Chem. C* **2008**, *112*, 11272−11279.

(32) Boardman, A. *Electromagnetic Surface Modes*; Wiley: Chichester, 1982.

(33) Scholl, J. A.; Koh, A. L.; Dionne, J. A. Quantum plasmon resonances of individual metallic nanoparticles. *Nature* **2012**, *483*, 421−428.

(34) Raza, S.; Stenger, N.; Kadkhodazadeh, S.; Fischer, S. V.; Kostesha, N.; Jauho, A.-P.; Burrows, A.; Wubs, M.; Mortensen, N. A. Blueshift of the surface plasmon resonance in silver nanoparticles studied with EELS. *Nanophotonics* **2013**, *2*, 131.

(35) Ciracì, C.; Hill, R. T.; Mock, J. J.; Urzhumov, Y.; Fernández-Domínguez, A. I.; Maier, S. A.; Pendry, J. B.; Chilkoti, A.; Smith, D. R. Probing the ultimate limits of plasmonic enhancement. *Science* **2012**, *337*, 1072−1074.

(36) Hajisalem, G.; Nezami, M. S.; Gordon, R. Probing the quantum tunneling limit of plasmonic enhancement by third harmonic generation. *Nano Lett.* **2014**, *14*, 6651−6654.

(37) Savage, K. J.; Hawkeye, M. M.; Esteban, R.; Borisov, A. G.; Aizpurua, J.; Baumberg, J. J. Revealing the quantum regime in tunnelling plasmonics. *Nature* **2012**, *491*, 574−577.

DOI: 10.1021/acsphotonics.5b00246
ACS Photonics 2015, 2, 987−992

(38) Scholl, J. A.; García-Etxarri, A.; Koh, A. L.; Dionne, J. A. Observation of Quantum Tunneling between Two Plasmonic Nanoparticles. *Nano Lett.* **2013**, *13*, 564−569.
(39) Zhu, W.; Crozier, K. B. Quantum mechanical limit to plasmonic enhancement as observed by surface-enhanced Raman scattering. *Nat. Commun.* **2014**, *5*, 5228.
(40) Romero, I.; Aizpurua, J.; Bryant, G. W.; García de Abajo, F. J. Plasmons in nearly touching metallic nanoparticles: Singular response in the limit of touching dimers. *Opt. Express* **2006**, *14*, 9988−9999.
(41) Lassiter, J. B.; Aizpurua, J.; Hernandez, L. I.; Brandl, D. W.; Romero, I.; Lal, S.; Hafner, J. H.; Nordlander, P.; Halas, N. J. Close encounters between two nanoshells. *Nano Lett.* **2008**, *8*, 1212−1218.
(42) Nordlander, P.; Oubre, C.; Prodan, E.; Li, K.; Stockman, M. I. Plasmon hybridizaton in nanoparticle dimers. *Nano Lett.* **2004**, *4*, 899−903.
(43) Pérez-González, O.; Zabala, N.; Borisov, A. G.; Halas, N. J.; Nordlander, P.; Aizpurua, J. Optical spectroscopy of conductive junctions in plasmonic cavities. *Nano Lett.* **2010**, *10*, 3090−3095.
(44) Pérez-González, O.; Aizpurua, J.; Zabala, N. Optical transport and sensing in plexcitonic nanocavities. *Opt. Express* **2013**, *21*, 15847−15858.
(45) Fontana, J.; Ratna, B. R. Highly tunable gold nanorod dimer resonances mediated through conductive junctions. *Appl. Phys. Lett.* **2014**, *105*, 01110710.1063/1.4887335
(46) Liu, L.; Wang, Y.; Fang, Z.; Zhao, K. Plasmon hybridization model generalized to conductively bridged nanoparticle dimers. *J. Chem. Phys.* **2013**, *139*, 064310.
(47) Wang, Y.; Li, Z.; Zhao, K.; Sobhani, A.; Zhu, X.; Fang, Z.; Halas, N. J. Substrate-mediated charge transfer plasmons in simple and complex nanoparticle clusters. *Nanoscale* **2013**, *5*, 9897−9901.
(48) Wu, L.; Duan, H.; Bai, P.; Bosman, M.; Yang, J. K. W.; Li, E. Fowler-Nordheim Tunneling Induced Charge Transfer Plasmons between Nearly Touching Nanoparticles. *ACS Nano* **2013**, *7*, 707−716.
(49) Song, P.; Nordlander, P.; Gao, S. Quantum mechanical study of the coupling of plasmon excitations to atomic-scale electron transport. *J. Chem. Phys.* **2011**, *134*, 074701.
(50) Song, P.; Meng, S.; Nordlander, P.; Gao, S. Quantum plasmonics: Symmetry-dependent plasmon-molecule coupling and quantized photoconductances. *Phys. Rev. B: Condens. Matter Mater. Phys.* **2012**, *86*, 121410.
(51) Thongrattanasiri, S.; Manjavacas, A.; Nordlander, P.; García de Abajo, F. J. Quantum junction plasmons in graphene dimers. *Laser Photon. Rev.* **2013**, *7*, 297−302.
(52) Benz, F.; Tserkezis, C.; Herrmann, L. O.; de Nijs, B.; Sanders, A.; Sigle, D. O.; Pukenas, L.; Evans, S. D.; Aizpurua, J.; Baumberg, J. J. Nanooptics of molecular-shunted plasmonic nanojunctions. *Nano Lett.* **2015**, *15*, 669−674.
(53) Tan, S. F.; Wu, L.; Yang, J. K. W.; Bai, P.; Bosman, M.; Nijhuis, C. A. Quantum plasmon resonances controlled by molecular tunnel junctions. *Science* **2014**, *343*, 1496−1499.
(54) Hohenberg, P.; Kohn, W. Inhomogeneous electron gas. *Phys. Rev.* **1964**, *136*, B864−B871.
(55) Kohn, W.; Sham, L. J. Self-consistent equations including exchange and correlation effects. *Phys. Rev.* **1965**, *140*, A1133−A1138.
(56) Runge, E.; Gross, E. K. U. Density-Functional Theory for Time-Dependent Systems. *Phys. Rev. Lett.* **1984**, *52*, 997−1000.
(57) Ceperley, D. M.; Alder, B. J. Ground state of the electron gas by a stochastic method. *Phys. Rev. Lett.* **1980**, *45*, 566−569.
(58) Perdew, J. P.; Zunger, A. Self-interaction correction to density-functional approximations for many-electron systems. *Phys. Rev. B: Condens. Matter Mater. Phys.* **1981**, *23*, 5048−5079.
(59) Pines, D.; Nozières, P. *The Theory of Quantum Liquids*; W. A. Benjamin, Inc.: New York, 1966.
(60) Li, Y.; Doak, P.; Kronik, L.; Neaton, J. B.; Natelson, D. Voltage tuning of vibrational mode energies in single-molecule junctions. *Proc. Natl. Acad. Sci. U. S. A.* **2014**, *111*, 1282−1287.
(61) Marinica, D.; Kazansky, A.; Nordlander, P.; Aizpurua, J.; Borisov, A. G. Quantum plasmonics: nonlinear effects in the field enhancement of a plasmonic nanoparticle dimer. *Nano Lett.* **2012**, *12*, 1333.

DOI: 10.1021/acsphotonics.5b00246
ACS Photonics 2015, 2, 987−992